BIOCHEMISTRY
including biophysical chemistry & molecular biology

Current Topic

pubs.acs.org/biochemistry

An Overview of Y-Family DNA Polymerases and a Case Study of Human DNA Polymerase η

Wei Yang*

Laboratory of Molecular Biology, National Institute of Diabetes and Digestive and Kidney Diseases, National Institutes of Health, Bethesda, Maryland 20892, United States

ABSTRACT: Y-Family DNA polymerases specialize in translesion synthesis, bypassing damaged bases that would otherwise block the normal progression of replication forks. Y-Family polymerases have unique structural features that allow them to bind damaged DNA and use a modified template base to direct nucleotide incorporation. Each Y-Family polymerase is unique and has different preferences for lesions to bypass and for dNTPs to incorporate. Y-Family polymerases are also characterized by a low catalytic efficiency, a low processivity, and a low fidelity on normal DNA. Recruitment of these specialized polymerases to replication forks is therefore regulated. The catalytic center of the Y-Family polymerases is highly conserved and homologous to that of high-fidelity and high-processivity DNA replicases. In this review, structural differences between Y-Family and A- and B-Family polymerases are compared and correlated with their functional differences. A time-resolved X-ray crystallographic study of the DNA synthesis reaction catalyzed by the Y-Family DNA polymerase human polymerase η revealed transient elements that led to the nucleotidyl-transfer reaction.

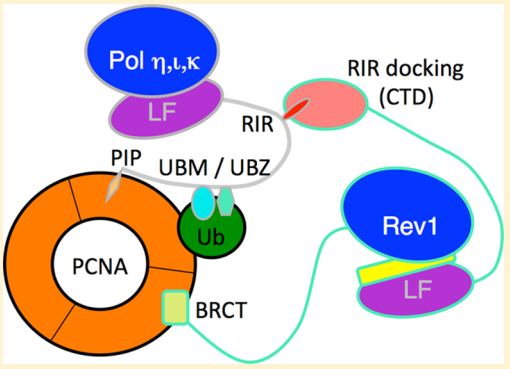

Replication of genomic DNA is a prerequisite for cell proliferation. High-fidelity DNA polymerases, regardless of their diversity in amino acid sequence, three-dimensional structure, origin, or complexity of subunit composition, are uniformly accurate and processive, such that up to billions of Watson−Crick (WC) base pairs are copied rapidly with high fidelity.[1−3] However, these remarkable high-speed and high-accuracy machines have an Achilles heel that is the intolerance of any alteration in the four normal bases, A, G, T, and C. The presence of a chemically modified DNA base or a DNA strand break could cause stalling or collapse of a replication fork. Because genomic DNA is frequently damaged by environmental toxins, radiation, and endogenous and exogenous metabolites,[4] every living organism relies on two general pathways to cope with "road blocks" in DNA replication.[5,6] One is to use specialized translesion DNA polymerases to accommodate DNA base lesions and continue DNA synthesis past damaged sites.[7−9] Alternatively, a detour by the homologous recombination pathway can avoid troublesome lesion sites and allow replication to proceed.[10,11]

DNA base lesions cause structural and chemical changes at the site of damage and inevitably hinder normal base pairing and base stacking in the vicinity, hence leading to general instability and distortion of the DNA double helix.[12−14] As a result, it is suggested that two different specialized polymerases are required to bypass a lesion in translesion DNA synthesis (TLS).[15] The first polymerase accommodates the damaged base and performs nucleotide incorporation directly opposite the lesion; the second polymerase extends the DNA primer beyond the lesion for several base pairs before the damaged DNA can be safely handled by a replicase (defined as a high-fidelity and high-processivity polymerase dedicated to the replication of normal DNA genomes). Y-Family polymerases are generally employed in the first step of TLS. For the second step of TLS, *Escherichia coli* DNA pol II and eukaryotic pol ζ, both of which belong to the B-Family, have been shown to perform primer extension after a lesion or a mismatched base pair.[16−18]

Because DNA lesions are varied in shape and chemical nature, a large fraction of DNA polymerases in each organism are specialized for repair and translesion synthesis, while replicases that copy genomic DNA of uniform WC base pairs consist of a relatively small fraction of polymerases in the genome. In *E. coli*, only one of the five total DNA polymerases is the high-fidelity and high-processivity replicase (pol III),[19] and the most abundant pol I has high fidelity, but low processivity, and performs short patch synthesis in DNA repair.[20] The remaining three, the Y-Family pol IV and pol V and the B-Family pol II, are involved in translesion and mutagenic DNA synthesis.[3,21−23] In humans, only five of 17 DNA polymerases are involved in normal genomic and mitochondrial DNA replication (pol α, δ, ε, and γ and telomerase). Of the remaining 12, four are Y-Family TLS polymerases [pol η, ι, κ, and Rev1 (see details below)], and eight others (pol β, λ, and μ, TdT, pol ν, θ, and ζ, and PrimPol) are required for TLS and repair of DNA breaks.[24−34]

Received: January 6, 2014
Revised: March 25, 2014
Published: April 10, 2014

dx.doi.org/10.1021/bi500019s | *Biochemistry* 2014, 53, 2793−2803

Individual Y-Family polymerases have different template base-binding sites and different preferences for the incoming nucleotide.[8,35] The general properties of Y-Family DNA polymerases are (1) the ability to conduct translesion synthesis with good accuracy, (2) a high error rate when copying normal DNA, (3) a lack of the 3′−5′ exonuclease activity and intrinsic proofreading ability,[36] (4) a low catalytic efficiency, and (5) a low processivity compared to that of DNA replicases.[9] The last two seemingly undesirable features ensure that they do not associate with or stay on a replication fork for more than several base pairs, which is thus advantageous in the scheme of DNA replication. The Y-Family polymerases are recruited to replication forks only when necessary. Regulation of their recruitment will be summarized in this review. For more comprehensive treatments, readers are referred to two recent reviews.[9,28] The focus of this review will be on the catalytic properties of Y-Family polymerases and comparisons with those of replicases.

Y-FAMILY POLYMERASES

Y-Family polymerases are divided into six major groups based on amino acid sequence. They are represented by *E. coli* pol IV (known as DinB) and pol V (of which UmuC is the catalytic subunit) and four human enzymes, pol *η*, *ι*, *κ*, and Rev1[7,9] (Figure 1A). All Y-Family polymerases comprise two functional parts, the polymerase catalytic region of 350−500 residues and a regulatory region from 10 (as in DinB, Dbh, and Dpo4) to 600 residues (as in Rev1).

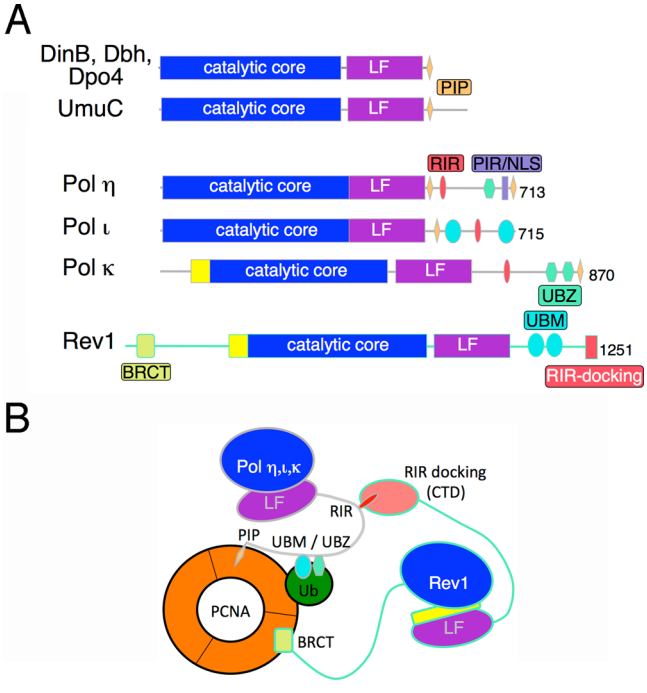

Figure 1. Diagram of domain structures and protein interactions of Y-Family polymerases. (A) Catalytic and regulatory regions of six subgroups of Y-Family polymerases. The catalytic core contains finger, palm, and thumb subdomains. LF denotes the little finger domain. PIP stands for the PCNA interaction peptide, RIR for the Rev1 interaction region, NLS for the nuclear localization signal, Ub for ubiquitin, UBZ for the Ub-binding zinc finger, UBM for the Ub-binding module, and BRCT for the BRCA1 C-terminal domain. (B) Schematic diagram of ubiquitinated PCNA interacting with all Y-Family polymerases and Rev1 interacting with pol *η*, *ι*, and *κ*.

Among these six groups, bacterial DinB and its archaeal homologues, Dpo4 and Dbh, are related to eukaryotic pol *κ* by sharing a structural gap in the catalytic region (Figure 2) and

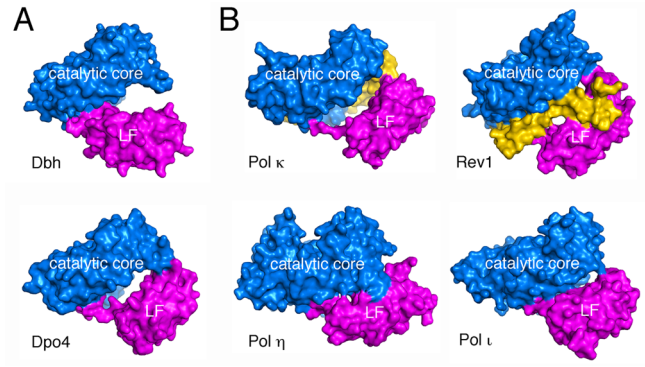

Figure 2. Varied interactions between the catalytic core (CC) and little finger domain (LF) of Y-Family polymerases. All structures shown here are of ternary complexes with DNA and dNTP. The CCs are superimposed, and the DNA and dNTP have been removed for clarity. (A) The relative orientation of CC (blue) and LF (purple) differs in archaeal Dbh [Protein Data Bank (PDB) entry 3BQ1] and Dpo4 (PDB entry 2AGQ), resulting a small gap between the CC and LF in Dpo4 and a large opening in Dbh. (B) The gap between the CC and LF is large in pol *κ* (PDB entry 2OH2) and Rev1 (PDB entry 2AQ4) and small to nonexistent in pol *η* (PDB entry 4ED8) and *ι* (PDB entry 3GV8). For the integrity of the catalytic region, pol *κ* uses its N-terminal extension (N-clasp, colored yellow) to bridge the CC and LF (in the back for this view), and Rev1 uses the N-terminal extension to fill the gap (crossing from the back to the front).

their tendency to make deletion mutation and ability to bypass bulky DNA adducts[8,37−39] (see details below). Initially, pol *η* and *ι* were considered close homologues,[40] but the two enzymes turn out to share little functional similarity.[9,41] Inactivation of POLH (the gene encoding pol *η*) in humans leads to extreme UV sensitivity and predisposition to skin cancers, and the genetic disease is known as the variant form of xeroderma pigmentosum (XPV);[42,43] however, the function of pol *ι* remains uncertain as *Poli*$^{-/-}$ and *Poli*$^{+/+}$ mice are alike in all aspects of growth.[44]

As the tenets of evolution would predict, the substrate specificity and prevalence of Y-Family polymerases are highly correlated with the abundance of naturally occurring DNA lesions. Ultraviolet radiation (UV) is an intrinsic part of sunlight, and UV-induced *cis-syn* pyrimidine dimers (cyclobutane pyrimidine dimers, or CPD) and 6-4 photoproducts are the oldest and most prevalent DNA lesions on earth.[45] Accordingly, UmuC, ubiquitous in bacteria, and pol *η*, found in all eukaryotes, primarily bypass UV-induced CPD lesions.[42,43,46] Because 6-4 photoproducts are efficiently removed by nucleotide excision repair, they are rarely encountered in the S phase. In addition, Rev1, which was originally identified and isolated because of its UV-induced expression and UV sensitivity in its absence,[47] is present universally among eukaryotes. Rev1 is a template-independent deoxycytidyl transferase and has more than 600 residues outside of the catalytic region (Figure 1).[48] The noncatalytic regions of Rev1 appear to regulate other Y-Family polymerases and contribute to TLS more than its catalytic activity.[49−52]

Polycyclic aromatic hydrocarbons (PAHs) are environmental pollutants produced by incomplete combustion of fossil fuels and biomass, and they are also present in tobacco smoke and

dx.doi.org/10.1021/bi500019s | *Biochemistry* 2014, 53, 2793−2803

Table 1. Structures of Y-Family DNA Polymerases

name	species	state	PDB entry
		Structures of the Catalytic Region	
Dpo4[a]	*Sulfolobus solfataricus*	apo	2RDI[100]
		DNA binary complex	2RDJ[100]
		ternary complex	1JX4, 2AGO;[95,136] 2ATL[137]
		frameshift	3QZ7, 3QZ8[39]
		CPD bypass	1RYR, 1RYS[138]
		BPDE bypass	1S0M;[138] 2IA6 and 2IBK[37]
		abasic bypass	1S0N, 1S0O, 1S10[105]
		[AF]G bypass	3KHG, 3KHH, 3KHL, 3KHR[139]
		APG bypass	4FBU, 4FBT[140]
		cisplatin bypass	3M9M, 3M9N, 3M9O[141]
		DFT bypass	2VA2, 2V9W[142]
		εdG (ε-G)	2BQR[143]
		PdG bypass	2R8I[144]
		8-oxo-G bypass	2ASD, 2ASJ, 2ASL;[137] 2C2D, 2C2E[66]
		8-oxo-G mispair	3GII, 3GIJ, 3GIK, 3GIL, 3GIM[145]
		8-oxo-G (mutant Dpo4)	2UVR, 2UVU, 2UVV, 2UVW[146]
Dbh	*Sulfolobus acidocaldarius*	apo	1IM4;[93] 1K1S[94]
		DNA binary complex	3BQ0, 3BQ2[38]
		ternary complex	3BQ1[38]
Dpo4–Dbh	chimera	ternary	4F4W, 4F4X, 4F4Y, 4F4Z, 4F50[86]
pol η	yeast	apo	1JIH[85]
	human	ternary complex	3MFH[67]
		CPD bypass	3MFI[67]
		cisplatin bypass	2R8K[96]
		8-oxo-G bypass	3OHA[67]
		DNA binary complex	4J9P, 4J9Q, 4J9R, 4J9S[99]
		ternary complex	4ED8[127]
		CPD bypass	3MR2, 3MR3[97]
		cisplatin bypass	4DL2, 4DL3, 4DL4, 4DL5, 4DL6, 4DL7;[98] 4EEY[147]
		T:G mismatch	4J9K, 4J9L, 4J9M, 4J9N, 4J9O, 4J9P, 4J9Q, 4J9R, 4J9S[98]
pol ι	human	ternary complex	2ALZ;[115] 3GV8[116]
		abasic bypass	3G6Y[148]
		8-oxo-G bypass	3Q8R[69]
		APG bypass	4EYI[149]
		εdA (ε-A)	2DPJ[150]
		T:G mismatch	3GV5, 3GV8;[116] 3H4B, 3H4D[118]
pol κ	human	apo	1T94[102]
		ternary complex	2OH2[103]
		CPD (extension)	3PZP[151]
		8-oxo-G bypass	2W7O, 2W7P;[152] 3IN5[153]
Rev1	yeast	ternary complex	2AQ4[106]
	human	ternary complex	3GQC[107]
		Structures of Regulatory Domains	
DinB	*E. coli* (PolIV)	LF (DinB) and β-clamp	1UNN[154]
Dpo4	*S. solfataricus*	Dpo4 and PCNA	3FDS[155]
pol η, ι, and κ	human	PIP (η, ι, or κ) and PCNA	2ZVK, 2ZVM, 2ZVL[156]
pol η	human	apo-UBZ	2I5O[157]
pol ι	human	apo-UBM2	2KHU;[158] 2L0G[159]
	mouse	UBM2–Ub	2KHW;[158] 2L0F[159]
		UBM1/2–Ub	2KWU, 2KWV[160]
Rev1	yeast	BRCT	4ID3;[161] 2M2I[73]
	mouse	apo CTD	2LSG[162]
	human	CTD-κ (RIR)	2LSJ[162]
		CTD-Rev3/7-κ (RIR)	4FJO[77]
		apo CTD	2LSY[163]
		CTD-η (RIR)	2LSK[163]
		CTD-Rev3/7	3VU7[76]
		CTD-Rev3/7-κ (RIR)	4GK5[78]

[a]There are additional structures in the PDB of Dpo4 complexed with DNA lesions beyond those listed here.

the human diet.[53] PAHs can form DNA base adducts, for example, benzo[*a*]pyrene, one of the earliest identified carcinogens.[54] Dpo4 and eukaryotic pol κ in particular are specialized to bypass these DNA bulky adducts.[37,55−61] Their close relative *E. coli* pol IV (DinB) bypasses N2-furfuryl-dG adducts efficiently.[62] Interestingly, the absence of pol κ in cell cultures also causes mild UV sensitivity, and pol κ has been shown to participate in excision repair of UV lesions.[63,64] In addition, 7,8-dihydro-8-oxyguanine (8-oxo-G) is a major oxidative lesion and promutagenic. Replicative DNA polymerases tend to incorporate dATP opposite an 8-oxo-G, resulting in a G → T transversion mutation.[65] Dpo4, pol η and ι, and presumably Rev1 are able to bypass 8-oxo-G with correct dCTP incorporation[66−71] (Table 1).

REGULATORY REGIONS OF Y-FAMILY POLYMERASES

Regulatory regions of Y-Family polymerases often contain a PCNA interacting peptide (PIP), a Rev1 interacting region (RIR), a ubiquitin-binding module (UBM), and a ubiquitin-binding zinc domain (UBZ)[8,9] (Figure 1). Rev1 is unique and has an N-terminal BRCT domain and a C-terminal protein-binding domain (Figure 1). Structural studies of these regulatory modules are mostly conducted by NMR as summarized in Table 1 and shown in Figure 3. Every Y-Family polymerase interacts with the replication processivity cofactor, β-sliding clamp in bacteria and PCNA in archaea and eukaryotes, via its PIP or BRCT domain (Rev1).[72,73] When DNA is damaged, PCNA becomes ubiquitinated,[74,75] and each eukaryotic Y-Family polymerase uses UBM or UBZ to interact with ubiquitin. In addition, human Y-Family polymerases η, ι, and κ each has an RIR that binds the C-terminal domain of

dx.doi.org/10.1021/bi500019s | *Biochemistry* 2014, 53, 2793−2803

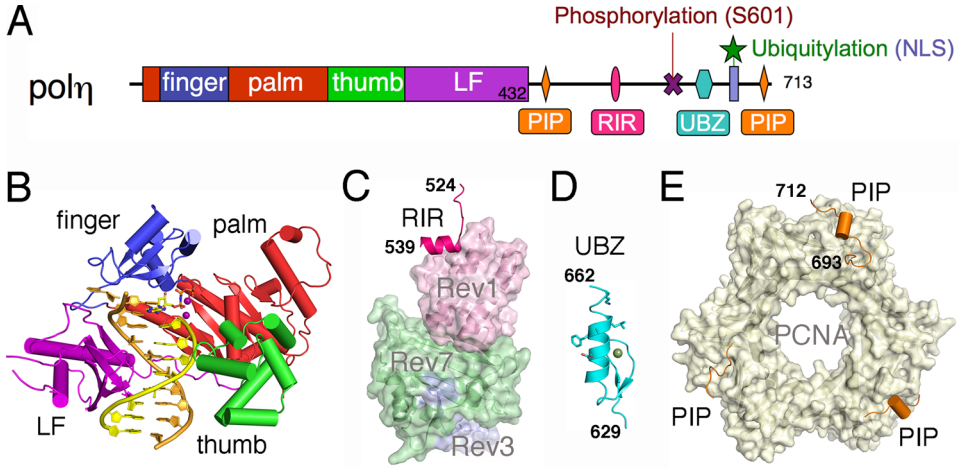

Figure 3. Structural domains in human pol η. (A) Diagram of the linear arrangement of functional domains in human pol η. Domains are color-coded. (B) Crystal structure of the catalytic region (amino acids 1−432) in a complex with DNA and dNTP (PDB entry 3MR2). (C) Structural model of the quaternary complex of pol η RIR complexed with the Rev1 CTD, Rev3, and Rev7. The model is a composite of RIR (η)−Rev1 (PDB entry 2LSK) and RIR(κ)−Rev1−Rev3−Rev7 complexes (PDB entry 4GK5). (D) NMR structure of the UBZ domain (PDB entry 2I5O) with the residues interacting with Ub shown as sticks. The Zn^{2+} ion is shown as a green sphere. (E) Crystal structure of human PCNA complexed with the pol η PIP (PDB entry 2ZVK). All parts of human pol η are shown as ribbon diagrams, and their interacting partners are shown as a molecular surface. The α-helices of pol η are shown as cylinders in panels B and E.

Rev1, which in turn interacts with Rev3 and Rev7 subunits of pol ζ.[51,76−78] Ubiquitinated PCNA and Rev1 appear to be the hubs of the TLS network.

Human pol η, whose inactivation directly leads to cancer,[79−82] is among the most scrutinized. In addition to the regulatory elements listed above, pol η itself can be ubiquitinated on a Lys residue within the nuclear localization signal (NLS) segment (Figure 3A), and this modification prevents the nearby PIP from interacting with PCNA[83] (Figure 1B). Pol η is also phosphorylated by ATR kinase upon UV irradiation (Figure 3A), which allows its TLS activity and checkpoint response to UV damage.[84]

A PREFORMED ACTIVE SITE OF Y-FAMILY POLYMERASES

The Y-Family polymerase catalytic region is composed of a conserved catalytic core, which includes the finger, palm, and thumb subdomains, and an appendage of the little finger domain.[8] The palm, finger, and thumb subdomains are found in all DNA polymerases. The "little finger" domain (LF), also known as the polymerase-associated domain (PAD),[85] is unique to the Y-Family and has more sequence variability than the catalytic core.[8,86] Three-dimensional structures of the catalytic region of a number of Y-Family polymerases from bacteria and archaea to humans have been reported (Table 1 and references therein). DNA substrate is bound between the thumb and LF. The palm subdomain contains the catalytic carboxylates that coordinate two Mg^{2+} ions, and the finger subdomain interacts with the template base and the incoming nucleotide (Figure 3).

In DNA polymerases other than the Y-Family members, the finger subdomain undergoes a large conformational change from an open state represented by apoproteins to a closed state adopted by the catalysis ready enzyme−DNA−dNTP ternary complexes[87−92] (Figure 4A,B). In contrast, the catalytic core of Y-Family polymerases contains a preformed active site with the finger closed in the absence of DNA, dNTP substrate, or both[85,93−95] (Figure 4C,D). Some Y-Family members can bind an incoming dNTP even in the absence of a base pair partner (templating base) and base stacking with the primer end.[96]

Correlated with being preformed, the active site of Y-Family members is large and solvent-exposed[8,67,97] (Figure 5). Thus, in a complete cycle of primer extension, from diffusion-in of dNTP and Mg^{2+} ions and the nucleotidyl-transfer reaction to pyrophosphate release and DNA translocation, no significant domain movement is needed or observed.[98−100] In contrast, the closed catalytic center of a replicative polymerase can accommodate only a WC base pair between a template base and an incoming dNTP and DNA and dNTP are constrained to the correct alignment for the nucleotidyl-transfer reaction.[88,101] The finger subdomain of a replicase has to open to release reaction product pyrophosphate and allow DNA to translocate and also a dNTP to bind for the next round of DNA synthesis (Figure 4A,B). The perfect alignment of a normal DNA and a correct dNTP in the active site of a replicative polymerase underlies its high fidelity and high catalytic efficiency. In contrast, the loose fit of substrates in Y-Family polymerases leads to a low fidelity, a low catalytic efficiency, and a low processivity of DNA synthesis.

LARGE CONFORMATIONAL CHANGES OF DPO4, DBH, AND POL κ

Substrate-dependent large conformational changes do occur in some Y-Family members. The catalytic core (CC) and little finger (LF) are connected by a flexible linker in all Y-Family polymerases. In the DinB subfamily, including Dpo4, Dbh, and pol κ, the CC and LF freely move relative to each other in the absence of DNA.[86,93,100,102] Large conformational changes are induced upon DNA binding.[86,100,103] Because of limited interactions between the CC and LF in Dpo4, Dbh, and pol κ, a large structural gap divides the CC and LF of these polymerases even in the ternary complexes with DNA and dNTP[8,97] (Figure 2). Pol κ depends on its N-terminal extension (N-clasp) to hold the CC and LF together[102,103] (Figures 1A and 2). The function of the structural gap in Dpo4, Dbh, and pol κ appears to accommodate minor groove bulky PAH adducts for lesion bypass[37,104] or nucleotides looped out

dx.doi.org/10.1021/bi500019s | Biochemistry 2014, 53, 2793−2803

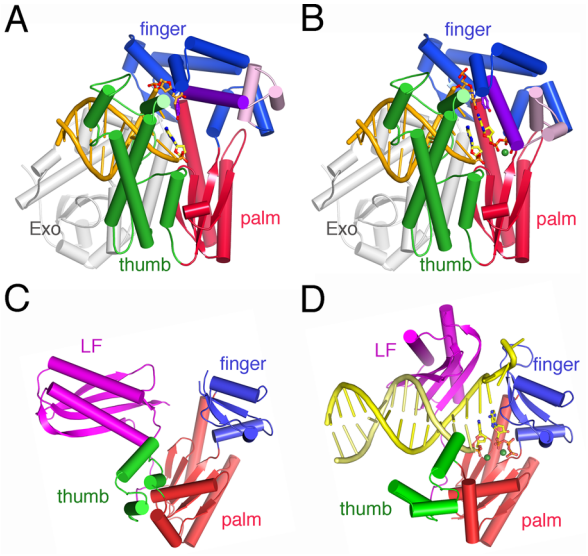

Figure 4. Different conformational changes in replicases and Y-Family polymerases. (A and B) Open (PDB entry 4BDP) and closed (PDB entry 3THV) structures, respectively, of *Bacillus* DNA polymerase I. The structure of the apo polymerase[135] is identical to the structure of a polymerase−DNA binary complex, and both have an open conformation. The "O" helix (colored deep purple) and the two surrounding helices (colored pink) undergo a "closing" motion upon binding of a correct incoming dNTP and metal ion (shown as a green sphere). (C and D) Structures of Dpo4 in apo (PDB entry 2RDI) and DNA-bound (PDB entry 2AGQ) forms, respectively. The little finger domain (LF) rotates nearly 130° between the two forms.

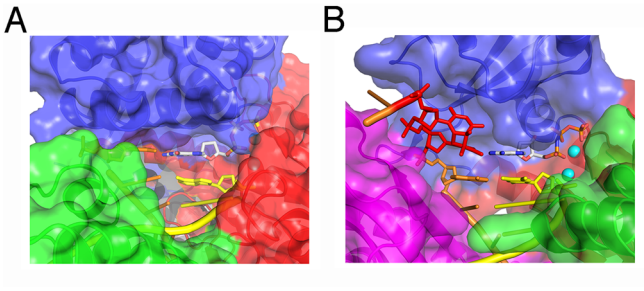

Figure 5. Comparison of the active site of a replicase and pol η. Close-up views of the ternary complexes of (A) T7 DNA polymerase (PDB entry 1T7P) and (B) pol η (PDB entry 3MR3). The finger (blue), palm (red), thumb (green), and LF (purple) domains are shown as ribbon diagrams superimposed with semitransparent molecular surfaces. DNA is shown as yellow (primer) and orange (template) tube and ladders; incoming dNTPs are shown as white sticks, and metal ions are shown as cyan spheres. The template base and catalytic metal ions in the T7 complex are barely visible, while the *cis-syn* thymine dimer (shown as red sticks), incoming nucleotide, and both active site metal ions in the pol η complex are solvent-exposed.

of a DNA template strand leading to a deletion frameshift.[38,39,105] Similarly, a large gap between the CC and LF of Rev1 is filled by the N-terminal extension from the catalytic core[106,107] (Figures 1A and 2). In human Rev1, the finger and thumb are connected by a long loop insertion, and the CC is ring-shaped and encircles the DNA substrate.[107]

In pol η, however, there is no structural gap and extensive interactions between the LF and the catalytic core stabilize the entire polymerase region (Figure 2). As a result, the apo pol η and DNA-bound complex structures are superimposable.[67,85,97]

The interactions between the CC and LF of pol η form a "molecular splint" to hold the template strand in the B-form even in the presence of a UV cross-linked *cis-syn* pyrimidine dimer.[97] With this "molecular splint", pol η is able to insert dAMPs across a *cis-syn* thymine dimer and also extend the primer for two more nucleotides,[97,108] so that the resulting TLS product can be utilized by a replicase to continue DNA synthesis.

The rate of DNA binding has not been reported for most of the Y-Family polymerases.[35] The poor affinity of Dbh for DNA[109] perhaps is due to its unique linker between the CC and LF[86] rather than the large conformational changes per se. It will be interesting to study whether the lack of CC−LF interaction in Dpo4 and pol κ slows DNA substrate binding compared to that of pol η, in which CC and LF do not undergo such conformational changes.

SUBSTRATE SELECTION AND LESION BYPASS SPECIFICITY

Since the structures of Dbh, Dpo4, and yeast pol η were determined 12 years ago, the unusually large and solvent-accessible active sites of Y-Family polymerases have been thought to underlie promiscuous lesion and dNTP selection. This notion has been supported by Dpo4's ability to bind and bypass many lesions (Table 1). Despite a generally enlarged replicating base pair-binding site, each Y-Family polymerase differs significantly in the size and shape of template base-binding site and has a different lesion preference. Pol η accommodates and accurately bypasses *cis-syn* pyrimidine dimers and also a 1,2-intrastrand d(GpG)−cisplatin cross-link[67,97,98] (Figure 5), but it is blocked by 6-4 photoproducts, BPDE−dG, and other bulky adducts.[110] Neither pol κ nor pol ι is capable of bypassing the 3′ base of a cross-linked base dimer. Likewise, only pol κ, and not pol η or pol ι, can accommodate the minor groove BPDE−dG adduct and accurately incorporates dCTP opposite the lesion.[55−57,59,60] To achieve this feat, pol κ depends on the flexibility between the catalytic core and little finger domain, the large structural gap, and its unique N-terminal extension (N-clasp).[103,104]

A couple of Y-Family polymerases have a specific preference for the incorporation of incorrect nucleotides, and the resulting mutations are sequence-specific. Pol η depends on two uniquely conserved residues (Arg61 and Gln38 in humans) for the accurate bypass of *cis-syn* pyrimidine dimers.[97,111] However, these two residues also play a key role in the efficient misincorporation of dGTP opposite a dT, particularly when the mismatched dT:dGTP replicating base pair is immediately preceded by an AT base pair,[99] in the DNA sequence called the WA motif. The misincorporation of dGTP by human pol η at the WA motif in undamaged DNA contributes to somatic hypermutation in the normal development process of the adaptive immune system.[112−114]

Rev1 uses an arginine side chain to form two hydrogen bonds with the base of a dCTP and to serve as a template for dCTP incorporation, while a DNA template base is flipped out of the active site.[106,107] The biological consequence of poly-dC synthesis remains unclear. In parallel, pol ι has a narrow binding site for the replicating base pair and thus favors the Hoogsteen base pair.[115,116] It is well-known that pol ι prefers to incorporate dGTP opposite template dT instead of the correct dATP.[40,117] However, crystal structures of pol ι show that an incoming dGTP and templating dT form neither a wobble nor a Hoogsteen base pair,[116,118] and the molecular mechanism of

dx.doi.org/10.1021/bi500019s | *Biochemistry* 2014, 53, 2793−2803

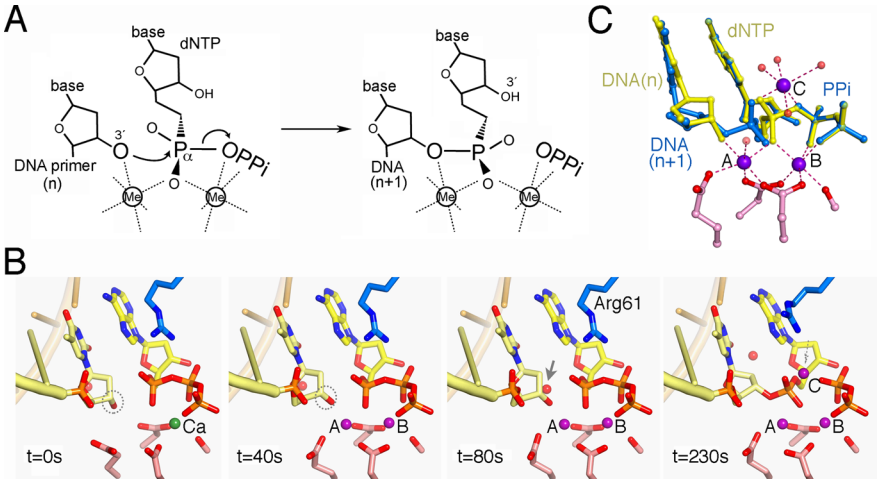

Figure 6. Nucleotidyl-transfer reaction. (A) Diagram of the reaction catalyzed by DNA polymerases. (B) Time-lapse recording of the reaction catalyzed by human pol η. At time zero, a Ca^{2+} ion occupied the B site, and the 3′ end of the primer (circled) is not aligned with the α-phosphate of dNTP. At 40 s (40 s after the addition of Mg^{2+}), both metal ion-binding sites A and B become occupied by Mg^{2+} ions, and the 3′-OH and α-phosphate are aligned. However, no chemical reaction is detected. At 80 s, a transient water appears (indicated by a gray arrowhead), and the new bond starts to form as indicated by the black double arrow. At 230 s, there are more products than substrate, and the third Mg^{2+} ion partially occupies the C site. (C) Composite of mixed substrate (colored yellow) and product (colored blue) in the middle of the reaction time course.

the preference of dGTP misincorporation over correct dATP incorporation remains unclear. Perhaps because of the lack of pol ι recruitment in the immune cells, *Poli*$^{-/-}$ mice do not exhibit altered somatic hypermutation as do *Pol*$\eta^{-/-}$ mice.

NUCLEOTIDYL-TRANSFER REACTION CATALYZED BY DNA POLYMERASES

All DNA polymerases, regardless of the structure and fidelity differences, catalyze the same nucleotidyl-transfer reaction, that is the formation of a new phosphodiester bond between the 3′-OH of a primer strand and the α-phosphate of an incoming dNTP, and concomitantly break the phosphodiester bond between the α- and β-phosphates of dNTP (Figure 6A). The reaction requires two Mg^{2+} ions in addition to a DNA template and primer and a dNTP,[8,24,119] and polymerases lower the energy barrier for product formation. All DNA polymerases contain two to three conserved carboxylates in the catalytic center. The Mg^{2+} ions neutralize the catalytic carboxylates and triphosphates of dNTP and facilitate the alignment of the substrates for the chemical reaction. The reaction is pH-dependent and analogous to acid−base catalysis, in which the nucleophile (3′-OH) needs to be deprotonated and the leaving group (pyrophosphate) needs to be protonated.[120] However, different from the classic acid−base catalysis in which conserved protein side chains serve as the general base and acid to extract and donate protons, DNA and RNA syntheses require two Mg^{2+} ions for the catalysis.[121,122]

Chemical reactions are heterogeneous because enzyme molecules are usually not synchronized. In addition, large conformational changes of many polymerases associated with each catalytic cycle easily obscure the small changes of chemical bond formation. Therefore, structural analyses of DNA polymerases were limited to static states of a homogeneous population. Crystal structures of a variety of DNA polymerases in complex with DNA and dNTP substrate have been reported,[24−26,89,92,119,123−125] where the nucleotidyl-transfer reaction was prevented by a nonreactive substrate, an inactivated polymerase, or the replacement of Mg^{2+} with Ca^{2+} because Ca^{2+} supports the formation of the enzyme−DNA−dNTP ternary complex but not the chemical reaction.[122] Crystal structures of polymerase−DNA product complexes are also available. However, how the actual nucleotidyl-transfer reaction takes place is still unclear.

TIME-RESOLVED CATALYSIS OF DNA SYNTHESIS BY POL η

In the course of our structural studies of pol η by X-ray crystallography, we noted that both substrate and product complexes of pol η coexisted in the same crystal lattice. Taking advantage of the absence of large conformational changes and slow reaction rates, we set out to record the course of the nucleotidyl-transer reaction catalyzed by pol η using time-resolved X-ray crystallography. To achieve this goal, it is necessary to turn off and turn on a chemical reaction at will. After our failed attempt to make a caged dNTP that can be activated by laser light,[126] we succeeded in growing crystals of native pol η with normal DNA and dNTP at pH 6.0, and with one Ca^{2+} per complex, no DNA synthesis took place.[127]

These crystals were soaked in stabilization buffers at pH 6.8−7.2 and continued to diffract X-rays to better than 2.0 Å resolution. Addition of 1 mM Mg^{2+} in the soaking buffer at pH 7.0 initiated the nucleotidyl-transfer reaction *in crystallo*. After Mg^{2+} exposure, at roughly 40 s intervals crystals were flash-cooled in liquid nitrogen to stop the chemical reaction, and the frozen samples at different reaction stages were analyzed by X-ray crystallography.

We found that binding of two Mg^{2+} ions was necessary to align the 3′-OH of the primer strand and the α-phosphate of dNTP (Figure 6B). With a single Ca^{2+} occupying the B metal-binding site, the 3′-OH together with the deoxyribose at the primer end was oriented away from the dNTP. After two Mg^{2+} ions had bound (at 40 s), the fully occupied A-site Mg^{2+} coordinated by the 3′-OH and the α-phosphate of dNTP led to the alignment of the reactants and tightening of the catalytic center. Interestingly, there was a delay between the presence of the well-aligned reactants and the formation of the new phosphodiester bond. The delay may correspond to a rate-limiting step observed in solution.[128]

Because the chemical reaction of the trillions of polymerase molecules in each crystal took place stochastically and at a different rate, when the new bond became detectable after Mg^{2+} exposure for 80 s, every crystal contained two mixed reaction species, the substrate and product (Figure 6B). With a diffraction resolution of 1.5−2.0 Å, the structures and proportions (occupancies) of the two reaction states of each crystal were readily refined. As the reaction progressed, the level of substrates decreased and the products accumulated. At 200 s, the crystals contained roughly equal amounts of the substrate and product immediately before and after the nucleotidyl-transfer reaction, and a composite of the two resembles the hypothesized pentacovalent phosphoryl-transfer reaction intermediate (Figure 6C). After 250 s, the two species seemed to reach equilibrium, with 70% being the product.

Our time-resolved study has revealed two transient elements in the chemical reaction. A water molecule, which formed a hydrogen bond with the 3′-OH, appeared at 80 s when the new bond started to form and disappeared at 200 s before the product peaked. This transient water was suspected to deprotonate the 3′-OH, but after substantial investigation, we found that this transient water is not the nominal general base because it can be replaced by a 2′-OH at the primer end without reducing the reaction rate.[127] Instead, a native dNTP may directly contribute to deprotonation of the 3′-OH because in the ternary complex of a nonreactive incoming nucleotide (dNMPNPP) a similar water molecule is stably bound to the 3′-OH without a chemical consequence.[97] The largest positional change in the transition from substrate to product occurred at the α-phosphorus of the incoming nucleotide, which moved 1.4 Å, and not the nucleophile 3′-O atom. It appears that the 3′-OH and dNTP held together by the two Mg^{2+} ions in the catalytic center may stochastically approach each other to be within such a critically short distance that the pK_a of the 3′-OH is reduced for the proton to leave readily. The transient water may be simply recruited to carry the proton away. In the absence of this particular water, such as in the case of the ribonucleotide substitution at the primer end, the proton may leave via 2′-OH to another water molecule. An alternative path of deprotonation of the 3′-OH has been proposed in dynamic simulation studies of three other DNA polymerases,[60,129,130] in which the proton leaves via the water coordinated by metal ion A to the end with the γ-phosphate of dNTP.

Among the two-Mg^{2+}-ion-dependent DNA polymerases, a conserved general base is absent, and there is likely no fixed path for the proton to depart. Instead, the two Mg^{2+} ions coordinated by the catalytic carboxylates perfectly align the primer end of DNA and dNTP, and the resulting electrostatic environment, including the contribution by the dNTP itself, likely reduces the pK_a of the 3′-OH for the nucleophilic attack to take place.

The second transient element observed in the *in crystallo* reaction catalyzed by pol η is a third Mg^{2+}. The third Mg^{2+}, which replaced the conserved Arg (Arg61) that neutralizes the dNTP, started to appear after 140 s when the products began to accumulate and its occupancy increased with an increase in the level of products (Figure 6B). Obviously, the +2 charged Mg^{2+} is more effective than the +1 charged Arg in neutralizing the locally accumulated negative charge in the transition states. This Mg^{2+} is coordinated by reaction products, primer$_{n+1}$, and pyrophosphate (Figure 6C). The nature of this transient divalent cation has been verified by using Mn^{2+} instead of Mg^{2+} in the reaction buffer. The third metal ion has also been observed in the time-resolved study of the X-Family DNA pol β.[131] In a related study of bacteriophage N4 RNA polymerase (A-Family), the third metal ion is not observed,[132] and its absence could be due to the lack of spatial (2.0 Å instead of 1.5−1.7 Å as in the studies of pol η and β) and temporal resolution, in which a reaction intermediate state was not recorded. In addition to neutralizing the excess negative charge of the reaction intermediates and stabilizing products, the third Mg^{2+} may play a role in protonating the pyrophosphate product.[127]

The two transient elements, the water and the third metal ion, revealed by time-resolved analyses have escaped notice in conventional studies of either enzyme−substrate or enzyme−product complexes. The third metal ion may be a general feature of DNA synthesis and many reactions catalyzed by the two-metal ion mechanism. The transient nature of the third metal ion may explain the discrepancy between "three metal ions" reported by chemical studies of the reaction process catalyzed by a group I intron and "two metal ions" observed in the crystal structures of ribozyme−substrate and ribozyme−product complexes.[133,134] The time-lapse series of the *in crystallo* reaction also reveals a delay between substrate and cofactor binding and the actual chemistry, during which a transient water molecule emerges to hydrogen bond with the 3′-OH. Deprotonation of the 3′-OH could be the rate-limiting step, and the details of what leads to its pK_a shift and the chemical reaction await future studies.

CONCLUDING REMARKS

In the 18 years since yeast Rev1 was first purified and shown to be a nucleotidyl-transferase, Y-Family DNA polymerases have been discovered and characterized. However, many questions are yet to be answered. The most fundamental question remaining is how so many DNA polymerases are coordinated at a replication fork to ensure that DNA synthesis occurs with the highest accuracy and efficiency in the presence of various roadblocks. The molecular details of how DNA polymerases switch when a lesion is encountered remain vague. With regard to the polymerase catalytic region, atomic structures of pol κ bypassing a BPDE adduct are yet to be obtained. While more protein modifications are likely to be found, the importance of the linear arrangement of PIP, RIR, UBM, and UBZ in each polymerase and whether these homologous functional parts can be exchanged between Y-Family members are not known.

AUTHOR INFORMATION

Corresponding Author

*E-mail: wei.yang@nih.gov. Telephone: (301) 402-4645. Fax: (301) 496-0201.

Funding

This work is funded by the National Institutes of Health Intramural Program (DK036146-07).

Notes

The authors declare no competing financial interest.

ACKNOWLEDGMENTS

I thank Drs. D. J. Leahy and R. Craigie for critical reading of the manuscript.

REFERENCES

(1) Kunkel, T. A. (2004) DNA replication fidelity. *J. Biol. Chem.* 279 (17), 16895−16898.

(2) Prindle, M. J., and Loeb, L. A. (2012) DNA polymerase δ in DNA replication and genome maintenance. *Environ. Mol. Mutagen. 53* (9), 666−682.
(3) Fijalkowska, I. J., Schaaper, R. M., and Jonczyk, P. (2012) DNA replication fidelity in *Escherichia coli*: A multi-DNA polymerase affair. *FEMS Microbiol. Rev. 36* (6), 1105−1121.
(4) Klarer, A. C., and McGregor, W. (2011) Replication of damaged genomes. *Crit. Rev. Eukaryotic Gene Expression 21* (4), 323−336.
(5) Budzowska, M., and Kanaar, R. (2009) Mechanisms of dealing with DNA damage-induced replication problems. *Cell Biochem. Biophys. 53* (1), 17−31.
(6) Boiteux, S., and Jinks-Robertson, S. (2013) DNA repair mechanisms and the bypass of DNA damage in *Saccharomyces cerevisiae*. *Genetics 193* (4), 1025−1064.
(7) Ohmori, H., et al. (2001) The Y-family of DNA polymerases. *Mol. Cell 8* (1), 7−8.
(8) Yang, W., and Woodgate, R. (2007) What a difference a decade makes: Insights into translesion DNA synthesis. *Proc. Natl. Acad. Sci. U.S.A. 104* (40), 15591−15598.
(9) Sale, J. E., Lehmann, A. R., and Woodgate, R. (2012) Y-family DNA polymerases and their role in tolerance of cellular DNA damage. *Nat. Rev. Mol. Cell Biol. 13* (3), 141−152.
(10) Muniandy, P. A., Liu, J., Majumdar, A., Liu, S. T., and Seidman, M. M. (2010) DNA interstrand crosslink repair in mammalian cells: Step by step. *Crit. Rev. Biochem. Mol. Biol. 45* (1), 23−49.
(11) Sale, J. E. (2012) Competition, collaboration and coordination: Determining how cells bypass DNA damage. *J. Cell Sci. 125* (Part 7), 1633−1643.
(12) Wood, R. D., et al. (2000) DNA damage recognition and nucleotide excision repair in mammalian cells. *Cold Spring Harbor Symp. Quant. Biol. 65*, 173−182.
(13) Yang, W. (2008) Structure and mechanism for DNA lesion recognition. *Cell Res. 18* (1), 184−197.
(14) Yang, W. (2006) Poor base stacking at DNA lesions may initiate recognition by many repair proteins. *DNA Repair 5* (6), 654−666.
(15) Livneh, Z., Ziv, O., and Shachar, S. (2010) Multiple two-polymerase mechanisms in mammalian translesion DNA synthesis. *Cell Cycle 9* (4), 729−735.
(16) Wang, F., and Yang, W. (2009) Structural insight into translesion synthesis by DNA Pol II. *Cell 139* (7), 1279−1289.
(17) Nelson, J. R., Gibbs, P. E., Nowicka, A. M., Hinkle, D. C., and Lawrence, C. W. (2000) Evidence for a second function for *Saccharomyces cerevisiae* Rev1p. *Mol. Microbiol. 37* (3), 549−554.
(18) Lee, Y. S., Gregory, M. T., and Yang, W. (2014) Human Pol ζ purified with accessary subunits is active in translesion DNA synthesis and complements Pol η in cisplatin bypass. *Proc. Natl. Acad. Sci. U.S.A. 111* (8), 2954−2959.
(19) McHenry, C. S. (2011) DNA replicases from a bacterial perspective. *Annu. Rev. Biochem. 80*, 403−436.
(20) Camps, M., and Loeb, L. A. (2004) When pol I goes into high gear: Processive DNA synthesis by pol I in the cell. *Cell Cycle 3* (2), 116−118.
(21) Hastings, P. J., et al. (2010) Competition of *Escherichia coli* DNA polymerases I, II and III with DNA Pol IV in stressed cells. *PLoS One 5* (5), e10862.
(22) Fuchs, R. P., Fujii, S., and Wagner, J. (2004) Properties and functions of *Escherichia coli*: Pol IV and Pol V. *Adv. Protein Chem. 69*, 229−264.
(23) Pham, P., Rangarajan, S., Woodgate, R., and Goodman, M. F. (2001) Roles of DNA polymerases V and II in SOS-induced error-prone and error-free repair in *Escherichia coli*. *Proc. Natl. Acad. Sci. U.S.A. 98* (15), 8350−8354.
(24) Moon, A. F., et al. (2007) The X family portrait: Structural insights into biological functions of X family polymerases. *DNA Repair 6* (12), 1709−1725.
(25) Beard, W. A., and Wilson, S. H. (2014) Structure and Mechanism of DNA Polymerase β. *Biochemistry 53*, DOI: 10.1021/bi500139h.
(26) Bebenek, K., Pedersen, L. C., and Kunkel, T. A. (2014) Structure−Function Studies of DNA Polymerase λ. *Biochemistry 53*, DOI: 10.1021/bi4017236.
(27) Yamtich, J., and Sweasy, J. B. (2010) DNA polymerase family X: Function, structure, and cellular roles. *Biochim. Biophys. Acta 1804* (5), 1136−1150.
(28) Sharma, S., Helchowski, C. M., and Canman, C. E. (2013) The roles of DNA polymerase ζ and the Y family DNA polymerases in promoting or preventing genome instability. *Mutat. Res. 743−744*, 97−110.
(29) Takata, K., Shimizu, T., Iwai, S., and Wood, R. D. (2006) Human DNA polymerase N (POLN) is a low fidelity enzyme capable of error-free bypass of 5S-thymine glycol. *J. Biol. Chem. 281* (33), 23445−23455.
(30) Yousefzadeh, M. J., and Wood, R. D. (2013) DNA polymerase POLQ and cellular defense against DNA damage. *DNA Repair 12* (1), 1−9.
(31) Garcia-Gomez, S., et al. (2013) PrimPol, an Archaic Primase/Polymerase Operating in Human Cells. *Mol. Cell 52* (4), 541−553.
(32) Bianchi, J., et al. (2013) PrimPol Bypasses UV Photoproducts during Eukaryotic Chromosomal DNA Replication. *Mol. Cell 52* (4), 566−573.
(33) Rudd, S. G., Glover, L., Jozwiakowski, S. K., Horn, D., and Doherty, A. J. (2013) PPL2 Translesion Polymerase Is Essential for the Completion of Chromosomal DNA Replication in the African Trypanosome. *Mol. Cell 52* (4), 554−565.
(34) Mouron, S., et al. (2013) Repriming of DNA synthesis at stalled replication forks by human PrimPol. *Nat. Struct. Mol. Biol. 20* (12), 1383−1389.
(35) Maxwell, B. A., and Suo, Z. (2014) Recent Insight into the Kinetic Mechanisms and Conformational Dynamics of Y-Family DNA Polymerases. *Biochemistry 53*, DOI: 10.1021/bi5000405.
(36) Reha-Krantz, L. J. (2010) DNA polymerase proofreading: Multiple roles maintain genome stability. *Biochim. Biophys. Acta 1804* (5), 1049−1063.
(37) Bauer, J., et al. (2007) A structural gap in Dpo4 supports mutagenic bypass of a major benzo[a]pyrene dG adduct in DNA through template misalignment. *Proc. Natl. Acad. Sci. U.S.A. 104* (38), 14905−14910.
(38) Wilson, R. C., and Pata, J. D. (2008) Structural insights into the generation of single-base deletions by the Y family DNA polymerase dbh. *Mol. Cell 29* (6), 767−779.
(39) Wu, Y., Wilson, R. C., and Pata, J. D. (2011) The Y-family DNA polymerase Dpo4 uses a template slippage mechanism to create single-base deletions. *J. Bacteriol. 193* (10), 2630−2636.
(40) McDonald, J. P., et al. (2001) DNA polymerase ι and related rad30-like enzymes. *Philos. Trans. R. Soc., B 356* (1405), 53−60.
(41) Waters, L. S., et al. (2009) Eukaryotic translesion polymerases and their roles and regulation in DNA damage tolerance. *Microbiol. Mol. Biol. Rev. 73* (1), 134−154.
(42) Masutani, C., et al. (1999) The XPV (xeroderma pigmentosum variant) gene encodes human DNA polymerase η. *Nature 399* (6737), 700−704.
(43) Johnson, R. E., Kondratick, C. M., Prakash, S., and Prakash, L. (1999) hRAD30 mutations in the variant form of xeroderma pigmentosum. *Science 285* (5425), 263−265.
(44) McDonald, J. P., et al. (2003) 129-derived strains of mice are deficient in DNA polymerase ι and have normal immunoglobulin hypermutation. *J. Exp. Med. 198* (4), 635−643.
(45) Cadet, J., Sage, E., and Douki, T. (2005) Ultraviolet radiation-mediated damage to cellular DNA. *Mutat. Res. 571* (1−2), 3−17.
(46) Tang, M., et al. (2000) Roles of *E. coli* DNA polymerases IV and V in lesion-targeted and untargeted SOS mutagenesis. *Nature 404* (6781), 1014−1018.
(47) Lawrence, C. W., and Christensen, R. B. (1978) Ultraviolet-induced reversion of cyc1 alleles in radiation-sensitive strains of yeast. I. rev1 mutant strains. *J. Mol. Biol. 122* (1), 1−21.

(48) Nelson, J. R., Lawrence, C. W., and Hinkle, D. C. (1996) Deoxycytidyl transferase activity of yeast REV1 protein. *Nature 382* (6593), 729−731.
(49) Guo, C., et al. (2003) Mouse Rev1 protein interacts with multiple DNA polymerases involved in translesion DNA synthesis. *EMBO J. 22* (24), 6621−6630.
(50) Ross, A. L., Simpson, L. J., and Sale, J. E. (2005) Vertebrate DNA damage tolerance requires the C-terminus but not BRCT or transferase domains of REV1. *Nucleic Acids Res. 33* (4), 1280−1289.
(51) Acharya, N., Johnson, R. E., Prakash, S., and Prakash, L. (2006) Complex formation with Rev1 enhances the proficiency of *Saccharomyces cerevisiae* DNA polymerase ζ for mismatch extension and for extension opposite from DNA lesions. *Mol. Cell. Biol. 26* (24), 9555−9563.
(52) Zhou, Y., Wang, J., Zhang, Y., and Wang, Z. (2010) The catalytic function of the Rev1 dCMP transferase is required in a lesion-specific manner for translesion synthesis and base damage-induced mutagenesis. *Nucleic Acids Res. 38* (15), 5036−5046.
(53) Phillips, D. H. (1999) Polycyclic aromatic hydrocarbons in the diet. *Mutat. Res. 443* (1−2), 139−147.
(54) Phillips, D. H. (1983) Fifty years of benzo(a)pyrene. *Nature 303* (5917), 468−472.
(55) Suzuki, N., et al. (2002) Translesion synthesis by human DNA polymerase κ on a DNA template containing a single stereoisomer of dG-(+)- or dG-(−)-anti-N(2)-BPDE (7,8-dihydroxy-anti-9,10-epoxy-7,8,9,10-tetrahydrobenzo[a]pyrene). *Biochemistry 41* (19), 6100−6106.
(56) Rechkoblit, O., et al. (2002) trans-Lesion synthesis past bulky benzo[a]pyrene diol epoxide N2-dG and N6-dA lesions catalyzed by DNA bypass polymerases. *J. Biol. Chem. 277* (34), 30488−30494.
(57) Huang, X., et al. (2003) Effects of base sequence context on translesion synthesis past a bulky (+)-trans-anti-B[a]P-N2-dG lesion catalyzed by the Y-family polymerase pol κ. *Biochemistry 42* (8), 2456−2466.
(58) Ling, H., et al. (2004) Crystal structure of a benzo[a]pyrene diol epoxide adduct in a ternary complex with a DNA polymerase. *Proc. Natl. Acad. Sci. U.S.A. 101* (8), 2265−2269.
(59) Xu, P., Oum, L., Geacintov, N. E., and Broyde, S. (2008) Nucleotide selectivity opposite a benzo[a]pyrene-derived N2-dG adduct in a Y-family DNA polymerase: A 5′-slippage mechanism. *Biochemistry 47* (9), 2701−2709.
(60) Lior-Hoffmann, L., et al. (2012) Preferred WMSA catalytic mechanism of the nucleotidyl transfer reaction in human DNA polymerase κ elucidates error-free bypass of a bulky DNA lesion. *Nucleic Acids Res. 40* (18), 9193−9205.
(61) Walsh, J. M., Ippoliti, P. J., Ronayne, E. A., Rozners, E., and Beuning, P. J. (2013) Discrimination against major groove adducts by Y-family polymerases of the DinB subfamily. *DNA Repair 12* (9), 713−722.
(62) Jarosz, D. F., Godoy, V. G., Delaney, J. C., Essigmann, J. M., and Walker, G. C. (2006) A single amino acid governs enhanced activity of DinB DNA polymerases on damaged templates. *Nature 439* (7073), 225−228.
(63) Schenten, D., et al. (2002) DNA polymerase κ deficiency does not affect somatic hypermutation in mice. *Eur. J. Immunol. 32* (11), 3152−3160.
(64) Ogi, T., et al. (2010) Three DNA polymerases, recruited by different mechanisms, carry out NER repair synthesis in human cells. *Mol. Cell 37* (5), 714−727.
(65) van Loon, B., Markkanen, E., and Hubscher, U. (2010) Oxygen as a friend and enemy: How to combat the mutational potential of 8-oxo-guanine. *DNA Repair 9* (6), 604−616.
(66) Zang, H., et al. (2006) Efficient and high fidelity incorporation of dCTP opposite 7,8-dihydro-8-oxodeoxyguanosine by *Sulfolobus solfataricus* DNA polymerase Dpo4. *J. Biol. Chem. 281* (4), 2358−2372.
(67) Silverstein, T. D., et al. (2010) Structural basis for the suppression of skin cancers by DNA polymerase η. *Nature 465* (7301), 1039−1043.
(68) Haracska, L., Yu, S. L., Johnson, R. E., Prakash, L., and Prakash, S. (2000) Efficient and accurate replication in the presence of 7,8-dihydro-8-oxoguanine by DNA polymerase η. *Nat. Genet. 25* (4), 458−461.
(69) Kirouac, K. N., and Ling, H. (2011) Unique active site promotes error-free replication opposite an 8-oxo-guanine lesion by human DNA polymerase ι. *Proc. Natl. Acad. Sci. U.S.A. 108* (8), 3210−3215.
(70) Maga, G., et al. (2007) 8-Oxo-guanine bypass by human DNA polymerases in the presence of auxiliary proteins. *Nature 447* (7144), 606−608.
(71) Zahn, K. E., Wallace, S. S., and Doublie, S. (2011) DNA polymerases provide a canon of strategies for translesion synthesis past oxidatively generated lesions. *Curr. Opin. Struct. Biol. 21* (3), 358−369.
(72) Guo, C., et al. (2006) REV1 protein interacts with PCNA: Significance of the REV1 BRCT domain in vitro and in vivo. *Mol. Cell 23* (2), 265−271.
(73) Pustovalova, Y., Maciejewski, M. W., and Korzhnev, D. M. (2013) NMR mapping of PCNA interaction with translesion synthesis DNA polymerase Rev1 mediated by Rev1-BRCT domain. *J. Mol. Biol. 425* (17), 3091−3105.
(74) Hoege, C., Pfander, B., Moldovan, G. L., Pyrowolakis, G., and Jentsch, S. (2002) RAD6-dependent DNA repair is linked to modification of PCNA by ubiquitin and SUMO. *Nature 419* (6903), 135−141.
(75) Lehmann, A. R. (2011) Ubiquitin-family modifications in the replication of DNA damage. *FEBS Lett. 585* (18), 2772−2779.
(76) Kikuchi, S., Hara, K., Shimizu, T., Sato, M., and Hashimoto, H. (2012) Structural basis of recruitment of DNA polymerase ζ by interaction between REV1 and REV7 proteins. *J. Biol. Chem. 287* (40), 33847−33852.
(77) Wojtaszek, J., et al. (2012) Structural basis of Rev1-mediated assembly of a quaternary vertebrate translesion polymerase complex consisting of Rev1, heterodimeric polymerase (Pol) ζ, and Pol κ. *J. Biol. Chem. 287* (40), 33836−33846.
(78) Xie, W., Yang, X., Xu, M., and Jiang, T. (2012) Structural insights into the assembly of human translesion polymerase complexes. *Protein Cell 3* (11), 864−874.
(79) Inui, H., et al. (2008) Xeroderma pigmentosum-variant patients from America, Europe, and Asia. *J. Invest. Dermatol. 128* (8), 2055−2068.
(80) Broughton, B. C., et al. (2002) Molecular analysis of mutations in DNA polymerase η in xeroderma pigmentosum-variant patients. *Proc. Natl. Acad. Sci. U.S.A. 99* (2), 815−820.
(81) Tanioka, M., et al. (2007) Molecular analysis of DNA polymerase η gene in Japanese patients diagnosed as xeroderma pigmentosum variant type. *J. Invest. Dermatol. 127* (7), 1745−1751.
(82) Opletalova, K., et al. (2014) Correlation of Phenotype/Genotype in a Cohort of 23 Xeroderma Pigmentosum-Variant Patients Reveals 12 New Disease-Causing POLH Mutations. *Hum. Mutat. 35* (1), 117−128.
(83) Bienko, M., et al. (2010) Regulation of translesion synthesis DNA polymerase η by monoubiquitination. *Mol. Cell 37* (3), 396−407.
(84) Gohler, T., Sabbioneda, S., Green, C. M., and Lehmann, A. R. (2011) ATR-mediated phosphorylation of DNA polymerase η is needed for efficient recovery from UV damage. *J. Cell Biol. 192* (2), 219−227.
(85) Trincao, J., et al. (2001) Structure of the catalytic core of *S. cerevisiae* DNA polymerase η: Implications for translesion DNA synthesis. *Mol. Cell 8* (2), 417−426.
(86) Wilson, R. C., Jackson, M. A., and Pata, J. D. (2013) Y-family polymerase conformation is a major determinant of fidelity and translesion specificity. *Structure 21* (1), 20−31.
(87) Li, Y., Korolev, S., and Waksman, G. (1998) Crystal structures of open and closed forms of binary and ternary complexes of the large fragment of *Thermus aquaticus* DNA polymerase I: Structural basis for nucleotide incorporation. *EMBO J. 17* (24), 7514−7525.
(88) Doublie, S., Sawaya, M. R., and Ellenberger, T. (1999) An open and closed case for all polymerases. *Structure 7* (2), R31−R35.

(89) Johnson, S. J., Taylor, J. S., and Beese, L. S. (2003) Processive DNA synthesis observed in a polymerase crystal suggests a mechanism for the prevention of frameshift mutations. *Proc. Natl. Acad. Sci. U.S.A. 100* (7), 3895−3900.
(90) Wang, W., Hellinga, H. W., and Beese, L. S. (2011) Structural evidence for the rare tautomer hypothesis of spontaneous mutagenesis. *Proc. Natl. Acad. Sci. U.S.A. 108* (43), 17644−17648.
(91) Kiefer, J. R., Mao, C., Braman, J. C., and Beese, L. S. (1998) Visualizing DNA replication in a catalytically active *Bacillus* DNA polymerase crystal. *Nature 391* (6664), 304−307.
(92) Xia, S., and Konigsberg, W. (2014) RB69 DNA Polymerase Structure, Kinetics, and Fidelity. *Biochemistry 53*, DOI: 10.1021/bi4014215.
(93) Zhou, B. L., Pata, J. D., and Steitz, T. A. (2001) Crystal structure of a DinB lesion bypass DNA polymerase catalytic fragment reveals a classic polymerase catalytic domain. *Mol. Cell 8* (2), 427−437.
(94) Silvian, L. F., Toth, E. A., Pham, P., Goodman, M. F., and Ellenberger, T. (2001) Crystal structure of a DinB family error-prone DNA polymerase from *Sulfolobus solfataricus*. *Nat. Struct. Biol. 8* (11), 984−989.
(95) Ling, H., Boudsocq, F., Woodgate, R., and Yang, W. (2001) Crystal structure of a Y-family DNA polymerase in action: A mechanism for error-prone and lesion-bypass replication. *Cell 107* (1), 91−102.
(96) Alt, A., et al. (2007) Bypass of DNA lesions generated during anticancer treatment with cisplatin by DNA polymerase *η*. *Science 318* (5852), 967−970.
(97) Biertumpfel, C., et al. (2010) Structure and mechanism of human DNA polymerase *η*. *Nature 465* (7301), 1044−1048.
(98) Zhao, Y., et al. (2012) Structural basis of human DNA polymerase *η*-mediated chemoresistance to cisplatin. *Proc. Natl. Acad. Sci. U.S.A. 109* (19), 7269−7274.
(99) Zhao, Y., et al. (2013) Mechanism of somatic hypermutation at the WA motif by human DNA polymerase *η*. *Proc. Natl. Acad. Sci. U.S.A. 110* (20), 8146−8151.
(100) Wong, J. H., Fiala, K. A., Suo, Z., and Ling, H. (2008) Snapshots of a Y-family DNA polymerase in replication: Substrate-induced conformational transitions and implications for fidelity of Dpo4. *J. Mol. Biol. 379* (2), 317−330.
(101) Kool, E. T. (2002) Active site tightness and substrate fit in DNA replication. *Annu. Rev. Biochem. 71*, 191−219.
(102) Uljon, S. N., et al. (2004) Crystal structure of the catalytic core of human DNA polymerase *κ*. *Structure 12* (8), 1395−1404.
(103) Lone, S., et al. (2007) Human DNA polymerase *κ* encircles DNA: Implications for mismatch extension and lesion bypass. *Mol. Cell 25* (4), 601−614.
(104) Liu, Y., et al. (2014) Variants of Mouse DNA Polymerase *κ* Reveal a Mechanism of Efficient and Accurate Translesion Synthesis Past a Benzo[a]pyrene dG Adduct. *Proc. Natl. Acad. Sci. U.S.A. 111* (5), 1789−1794.
(105) Ling, H., Boudsocq, F., Woodgate, R., and Yang, W. (2004) Snapshots of replication through an abasic lesion; structural basis for base substitutions and frameshifts. *Mol. Cell 13* (5), 751−762.
(106) Nair, D. T., Johnson, R. E., Prakash, L., Prakash, S., and Aggarwal, A. K. (2005) Rev1 employs a novel mechanism of DNA synthesis using a protein template. *Science 309* (5744), 2219−2222.
(107) Swan, M. K., Johnson, R. E., Prakash, L., Prakash, S., and Aggarwal, A. K. (2009) Structure of the human Rev1-DNA-dNTP ternary complex. *J. Mol. Biol. 390* (4), 699−709.
(108) McCulloch, S. D., et al. (2004) Preferential cis-syn thymine dimer bypass by DNA polymerase *η* occurs with biased fidelity. *Nature 428* (6978), 97−100.
(109) Cramer, J., and Restle, T. (2005) Pre-steady-state kinetic characterization of the DinB homologue DNA polymerase of *Sulfolobus solfataricus*. *J. Biol. Chem. 280* (49), 40552−40558.
(110) Masutani, C., Kusumoto, R., Iwai, S., and Hanaoka, F. (2000) Mechanisms of accurate translesion synthesis by human DNA polymerase *η*. *EMBO J. 19* (12), 3100−3109.
(111) Suarez, S. C., Beardslee, R. A., Toffton, S. M., and McCulloch, S. D. (2013) Biochemical analysis of active site mutations of human polymerase *η*. *Mutat. Res. 745−746*, 46−54.
(112) Zeng, X., et al. (2001) DNA polymerase *η* is an A-T mutator in somatic hypermutation of immunoglobulin variable genes. *Nat. Immunol. 2* (6), 537−541.
(113) Faili, A., et al. (2004) DNA polymerase *η* is involved in hypermutation occurring during immunoglobulin class switch recombination. *J. Exp. Med. 199* (2), 265−270.
(114) Zeng, X., Negrete, G. A., Kasmer, C., Yang, W. W., and Gearhart, P. J. (2004) Absence of DNA polymerase *η* reveals targeting of C mutations on the nontranscribed strand in immunoglobulin switch regions. *J. Exp. Med. 199* (7), 917−924.
(115) Nair, D. T., Johnson, R. E., Prakash, L., Prakash, S., and Aggarwal, A. K. (2005) Human DNA polymerase *ι* incorporates dCTP opposite template G via a G·C$^+$ Hoogsteen base pair. *Structure 13* (10), 1569−1577.
(116) Kirouac, K. N., and Ling, H. (2009) Structural basis of error-prone replication and stalling at a thymine base by human DNA polymerase *ι*. *EMBO J. 28* (11), 1644−1654.
(117) Zhang, Y., Yuan, F., Wu, X., and Wang, Z. (2000) Preferential incorporation of G opposite template T by the low-fidelity human DNA polymerase *ι*. *Mol. Cell. Biol. 20* (19), 7099−7108.
(118) Jain, R., et al. (2009) Replication across template T/U by human DNA polymerase *ι*. *Structure 17* (7), 974−980.
(119) Jager, J., and Pata, J. D. (1999) Getting a grip: Polymerases and their substrate complexes. *Curr. Opin. Struct. Biol. 9* (1), 21−28.
(120) Castro, C., et al. (2007) Two proton transfers in the transition state for nucleotidyl transfer catalyzed by RNA- and DNA-dependent RNA and DNA polymerases. *Proc. Natl. Acad. Sci. U.S.A. 104* (11), 4267−4272.
(121) Steitz, T. A., and Steitz, J. A. (1993) A general two-metal-ion mechanism for catalytic RNA. *Proc. Natl. Acad. Sci. U.S.A. 90* (14), 6498−6502.
(122) Yang, W., Lee, J. Y., and Nowotny, M. (2006) Making and breaking nucleic acids: Two-Mg^{2+}-ion catalysis and substrate specificity. *Mol. Cell 22* (1), 5−13.
(123) Berman, A. J., et al. (2007) Structures of *ϕ*29 DNA polymerase complexed with substrate: The mechanism of translocation in B-family polymerases. *EMBO J. 26* (14), 3494−3505.
(124) Franklin, M. C., Wang, J., and Steitz, T. A. (2001) Structure of the replicating complex of a pol *α* family DNA polymerase. *Cell 105* (5), 657−667.
(125) Evans, R. J., et al. (2008) Structure of PolC reveals unique DNA binding and fidelity determinants. *Proc. Natl. Acad. Sci. U.S.A. 105* (52), 20695−20700.
(126) Schlichting, I., et al. (1990) Time-resolved X-ray crystallographic study of the conformational change in Ha-Ras p21 protein on GTP hydrolysis. *Nature 345* (6273), 309−315.
(127) Nakamura, T., Zhao, Y., Yamagata, Y., Hua, Y. J., and Yang, W. (2012) Watching DNA polymerase *η* make a phosphodiester bond. *Nature 487* (7406), 196−201.
(128) Showalter, A. K., and Tsai, M. D. (2002) A reexamination of the nucleotide incorporation fidelity of DNA polymerases. *Biochemistry 41* (34), 10571−10576.
(129) Wang, L., Yu, X., Hu, P., Broyde, S., and Zhang, Y. (2007) A water-mediated and substrate-assisted catalytic mechanism for *Sulfolobus solfataricus* DNA polymerase IV. *J. Am. Chem. Soc. 129* (15), 4731−4737.
(130) Wang, L., Broyde, S., and Zhang, Y. (2009) Polymerase-tailored variations in the water-mediated and substrate-assisted mechanism for nucleotidyl transfer: Insights from a study of T7 DNA polymerase. *J. Mol. Biol. 389* (4), 787−796.
(131) Freudenthal, B. D., Beard, W. A., Shock, D. D., and Wilson, S. H. (2013) Observing a DNA polymerase choose right from wrong. *Cell 154* (1), 157−168.
(132) Basu, R. S., and Murakami, K. S. (2013) Watching the bacteriophage N4 RNA polymerase transcription by time-dependent

soak-trigger-freeze X-ray crystallography. *J. Biol. Chem. 288* (5), 3305−3311.
(133) Shan, S., Yoshida, A., Sun, S., Piccirilli, J. A., and Herschlag, D. (1999) Three metal ions at the active site of the *Tetrahymena* group I ribozyme. *Proc. Natl. Acad. Sci. U.S.A. 96* (22), 12299−12304.
(134) Stahley, M. R., and Strobel, S. A. (2005) Structural evidence for a two-metal-ion mechanism of group I intron splicing. *Science 309* (5740), 1587−1590.
(135) Kiefer, J. R., et al. (1997) Crystal structure of a thermostable *Bacillus* DNA polymerase I large fragment at 2.1 Å resolution. *Structure 5* (1), 95−108.
(136) Vaisman, A., Ling, H., Woodgate, R., and Yang, W. (2005) Fidelity of Dpo4: Effect of metal ions, nucleotide selection and pyrophosphorolysis. *EMBO J. 24* (17), 2957−2967.
(137) Rechkoblit, O., et al. (2006) Stepwise translocation of Dpo4 polymerase during error-free bypass of an oxoG lesion. *PLoS Biol. 4* (1), e11.
(138) Ling, H., Boudsocq, F., Plosky, B. S., Woodgate, R., and Yang, W. (2003) Replication of a cis-syn thymine dimer at atomic resolution. *Nature 424* (6952), 1083−1087.
(139) Rechkoblit, O., et al. (2010) Mechanism of error-free and semitargeted mutagenic bypass of an aromatic amine lesion by Y-family polymerase Dpo4. *Nat. Struct. Mol. Biol. 17* (3), 379−388.
(140) Kirouac, K. N., Basu, A. K., and Ling, H. (2013) Structural mechanism of replication stalling on a bulky amino-polycyclic aromatic hydrocarbon DNA adduct by a Y family DNA polymerase. *J. Mol. Biol. 425* (22), 4167−4176.
(141) Wong, J. H., et al. (2010) Structural insight into dynamic bypass of the major cisplatin-DNA adduct by Y-family polymerase Dpo4. *EMBO J. 29* (12), 2059−2069.
(142) Irimia, A., Eoff, R. L., Pallan, P. S., Guengerich, F. P., and Egli, M. (2007) Structure and activity of Y-class DNA polymerase DPO4 from *Sulfolobus solfataricus* with templates containing the hydrophobic thymine analog 2,4-difluorotoluene. *J. Biol. Chem. 282* (50), 36421−36433.
(143) Zang, H., et al. (2005) DNA adduct bypass polymerization by *Sulfolobus solfataricus* DNA polymerase Dpo4: Analysis and crystal structures of multiple base pair substitution and frameshift products with the adduct 1,N2-ethenoguanine. *J. Biol. Chem. 280* (33), 29750−29764.
(144) Wang, Y., et al. (2008) Insertion of dNTPs opposite the 1,N2-propanodeoxyguanosine adduct by *Sulfolobus solfataricus* P2 DNA polymerase IV. *Biochemistry 47* (28), 7322−7334.
(145) Rechkoblit, O., et al. (2009) Impact of conformational heterogeneity of OxoG lesions and their pairing partners on bypass fidelity by Y family polymerases. *Structure 17* (5), 725−736.
(146) Eoff, R. L., Irimia, A., Angel, K. C., Egli, M., and Guengerich, F. P. (2007) Hydrogen bonding of 7,8-dihydro-8-oxodeoxyguanosine with a charged residue in the little finger domain determines miscoding events in *Sulfolobus solfataricus* DNA polymerase Dpo4. *J. Biol. Chem. 282* (27), 19831−19843.
(147) Ummat, A., et al. (2012) Structural basis for cisplatin DNA damage tolerance by human polymerase *η* during cancer chemotherapy. *Nat. Struct. Mol. Biol. 19* (6), 628−632.
(148) Nair, D. T., Johnson, R. E., Prakash, L., Prakash, S., and Aggarwal, A. K. (2009) DNA synthesis across an abasic lesion by human DNA polymerase *ι*. *Structure 17* (4), 530−537.
(149) Kirouac, K. N., Basu, A. K., and Ling, H. (2013) Replication of a carcinogenic nitropyrene DNA lesion by human Y-family DNA polymerase. *Nucleic Acids Res. 41* (3), 2060−2071.
(150) Nair, D. T., Johnson, R. E., Prakash, L., Prakash, S., and Aggarwal, A. K. (2006) Hoogsteen base pair formation promotes synthesis opposite the 1,N6-ethenodeoxyadenosine lesion by human DNA polymerase *ι*. *Nat. Struct. Mol. Biol. 13* (7), 619−625.
(151) Vasquez-Del Carpio, R., et al. (2011) Role of human DNA polymerase *κ* in extension opposite from a cis-syn thymine dimer. *J. Mol. Biol. 408* (2), 252−261.
(152) Irimia, A., Eoff, R. L., Guengerich, F. P., and Egli, M. (2009) Structural and functional elucidation of the mechanism promoting error-prone synthesis by human DNA polymerase *κ* opposite the 7,8-dihydro-8-oxo-2′-deoxyguanosine adduct. *J. Biol. Chem. 284* (33), 22467−22480.
(153) Vasquez-Del Carpio, R., et al. (2009) Structure of human DNA polymerase *κ* inserting dATP opposite an 8-oxoG DNA lesion. *PLoS One 4* (6), e5766.
(154) Bunting, K. A., Roe, S. M., and Pearl, L. H. (2003) Structural basis for recruitment of translesion DNA polymerase Pol IV/DinB to the *β*-clamp. *EMBO J. 22* (21), 5883−5892.
(155) Xing, G., Kirouac, K., Shin, Y. J., Bell, S. D., and Ling, H. (2009) Structural insight into recruitment of translesion DNA polymerase Dpo4 to sliding clamp PCNA. *Mol. Microbiol. 71* (3), 678−691.
(156) Hishiki, A., et al. (2009) Structural basis for novel interactions between human translesion synthesis polymerases and proliferating cell nuclear antigen. *J. Biol. Chem. 284* (16), 10552−10560.
(157) Bomar, M. G., Pai, M. T., Tzeng, S. R., Li, S. S., and Zhou, P. (2007) Structure of the ubiquitin-binding zinc finger domain of human DNA Y-polymerase *η*. *EMBO Rep. 8* (3), 247−251.
(158) Bomar, M. G., et al. (2010) Unconventional ubiquitin recognition by the ubiquitin-binding motif within the Y family DNA polymerases *ι* and Rev1. *Mol. Cell 37* (3), 408−417.
(159) Cui, G., et al. (2010) Structural basis of ubiquitin recognition by translesion synthesis DNA polymerase *ι*. *Biochemistry 49* (47), 10198−10207.
(160) Burschowsky, D., et al. (2011) Structural analysis of the conserved ubiquitin-binding motifs (UBMs) of the translesion polymerase *ι* in complex with ubiquitin. *J. Biol. Chem. 286* (2), 1364−1373.
(161) Pryor, J. M., Gakhar, L., and Washington, M. T. (2013) Structure and functional analysis of the BRCT domain of translesion synthesis DNA polymerase Rev1. *Biochemistry 52* (1), 254−263.
(162) Wojtaszek, J., et al. (2012) Multifaceted recognition of vertebrate Rev1 by translesion polymerases *ζ* and *κ*. *J. Biol. Chem. 287* (31), 26400−26408.
(163) Pozhidaeva, A., et al. (2012) NMR structure and dynamics of the C-terminal domain from human Rev1 and its complex with Rev1 interacting region of DNA polymerase *η*. *Biochemistry 51* (27), 5506−5520.